MEASUREMENT AND CALCULATION OF BORE PROPAGATION IN MEANDERING RIVER

DAISUKE KOBAYASHI
Hiroshima University, Higashi-hiroshima, Japan, m186794@hiroshima-u.ac.jp

TATSUHIKO UCHIDA
Hiroshima University, Higashi-hiroshima, Japan, utida@hiroshima-u.ac.jp

YOSHIHISA KAWAHARA
Hiroshima University, Higashi-hiroshima, Japan, kawahr@hiroshima-u.ac.jp

ABSTRACT

Tsunami run-up in rivers can be classified into two forms: breaking bore and undular bore. In this study, focusing on the breaking bore, we investigated hydraulic bore propagations by rapidly opening a gate installed in a straight and meandering channel. We measured the temporal variations in wave height and compared the experimental results and calculation results in the straight and meandering channels with the aim of clarifying the characteristics of bore propagation. We generated the two type of bores in our experiment; Type 1 is the breaking bore with downstream water depth close to dry, Type 2 is the breaking bore on wet bed. We calculated the bore propagation in the meandering channel using a two-dimensional shallow water equation. By comparing the wave height of the meandering channel in the calculation and the experiment results, we found that the two-dimensional calculation results of the breaking bore can substantially express the wave height variations of Type 2 in a meandering channel. On the other hand, it was investigated on the Type 1 breaking bore in the meandering channel that some waves propagated to upstream direction under supercritical flow condition due to the reflection from the side bank that cannot be reproduced by the shallow water equation.

Keywords: breaking bore, shallow water equation, three-dimensionality

1. INTRODUCTION

Tsunami run-up was investigated not only on land but also in many rivers when the Great East Japan Earthquake occurred in 2011. Tanaka et al. (2013) investigated the interactions between tsunami run-up in rivers and tsunami inundation. They found that the tsunami came from both directions making it evacuation difficult and overtopping the flow; erosion marks were mainly found on the outer bank. An analytical method that can adequately assess tsunami run-up in rivers is needed to reduce tsunami damage.

Many studies on bores and dam-break flows have been conducted to develop the method.

Guido et al. (1998) indicated that the front of the positive and negative bore results obtained from the characteristic equation roughly agree with experimental results in the horizontal channel. Cagatay et al. (2008) carried out an experiment on the dam-break flow generated by opening a gate. They indicated that the dam break flow form was affected by the initial downstream water depth, and Ritter and Stoker's analytical solution of wave speed was larger than their experimental value. Liu (2017) generated dam-break flows under different conditions of the initial upstream and downstream water depths and measured temporal variations in wave height and velocity in the downstream channel. They showed that temporal variations are affected by the differences in water depth between the upstream and downstream of the gate, and the duration time, in which the wave height keeps a maximum value, is dependent on the length of the water tank upstream.

As described above, there have been many studies on bores in a straight channel. However, many rivers near coastal lines in which bores are actually propagated are meandering. This makes it difficult to apply the results obtained from the studies on bores or dam-break flows in straight channels to tsunami run-up in rivers.

A few experiments and numerical calculations have been carried out for non-straight channels.

The study of bores in curved channels was studied by Goto et al. (1981) and Sky Miller et al. (1989). They compared the experimental values of wave height to the calculation results obtained by two-dimensional shallow water equations. However, the main objective was to validate the numerical calculation method. Therefore, the propagation of bores in curved channels was not discussed in detail.

Soares et al. (2002) applied a hybrid one-/two-dimensional approach to dam-break flows in sharp 90° bends. In this approach, the 2D model is applied only to the bent part, and the 1D model is applied to the other straight part. It can reproduce the bore propagation in the upstream direction, while the front arrival time downstream from the bend is less accurate.

However, the effect of the channel meander of rivers on the increasing wave height is still quite unclear. A few studies have been conducted on bores in meandering channels.

Yung et al. (1979) conducted an experiment on the dam-break flow in a meandering channel that illustrated the difference in the maximum wave heights of the straight and meandering channels. Ito et al. (2014) measured the water level of bores in a meandering channel; however, the bed slope is much larger than that of rivers on land.

In this study, we conduct an experiment on the breaking bore in straight and meandering channels. We aim to clarify the propagation characteristics of bores in meandering channels and validate a numerical analysis method for tsunami run-up in rivers by comparing the experimental results of the wave height variation in straight and meandering channels to the calculation results of the shallow water equation.

2. EXPERIMENTAL SET UP

Figure 1 shows the experimental channel. The experimental channel consists of a straight channel and a meandering channel. The length and width of the straight channel are 16.1 m and 0.40 m, respectively. The horizontal distance, channel width, meander wavelength, meander length, and sinuosity of the meandering channel are 16.1 m, 0.39 m, 6.43 m, and 8.06 m, and 1.25, respectively, and the maximum deflection angle is 53.0 (°). The bed slope of this channel is 0. The meandering shape of the channel is represented by equation (1).

$$\theta = \theta_{\max} \sin \frac{2\pi s}{L} \tag{1}$$

Here, s =river road distance, θ=deflection angle (°), L =meander length, θ_{max} =maximum deflection angle. We designed a meandering channel in reference to rivers where the tsunami run-up was confirmed in the Great East Japan Earthquake on March 11, 2011. We generate the bore to open the gate rapidly. The gate is installed 1.68 m away from the upstream end. Table 1 shows the experimental conditions. Here, ω =wave front speed, h=downstream water depth. A breaking bore is generated by varying the ratio of the water level upstream and downstream the gate (Nakagawa et al., 1969). Six measurement points and sections are installed in the straight channel and meandering channel, respectively, such that the respective distances between the straight channel and meandering channel and the gate are equal. Two measurement points are set near both banks in each measurement section. We measure the wave height variation of bores using the servo type wave height meter. The instrument consists of the 7cm wide main body and the expandable wave prove. The measurement point of Type 2 is at 2.0 cm from the bank. However, owing to the expansion limit of the probe, we must install the main body at the position lower than the top of the bank when we measure Type 1 wave height. Therefore, the measurement point of Type 1 is at 3.5cm (a half of main body width) from the bank. That's why the distance between the measuring points and bank differs for each experimental condition. Using the minimum, maximum, and mean values of the deflection angle, we determine the measurement cross sections.

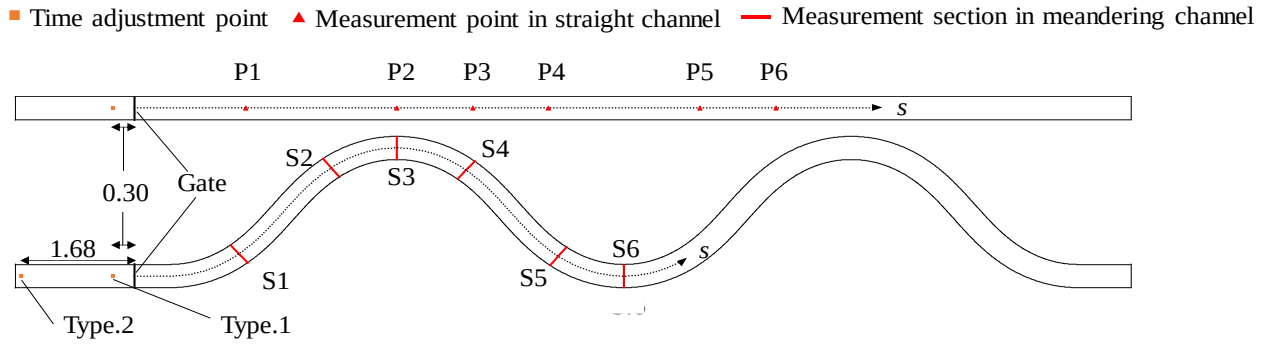

Figure 1. Plan of experimental channel (unit: m)

Table 1. Experimental conditions

	Type 1	*Type 2*
Upstream water depth(m)	0.300	0.285
Downstream water depth(m)	0.020	0.107
Water depth ratio	0.0667	0.375
Fruide number $(=\omega/\sqrt{gh})$	4.11	1.62

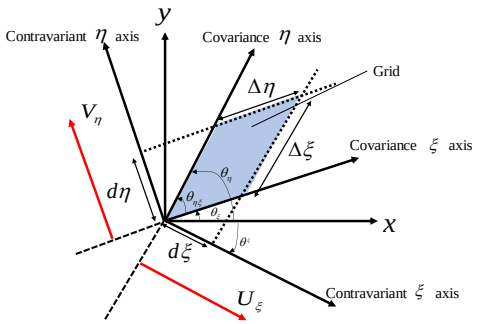

Figure 2. Geometric display in a general coordinate system (Watanabe et al., 2002)

The positive bore propagates downstream because of the rapid opening of the gate, whereas the negative bore propagates upstream. We install the measurement point of the negative bore upstream from the gate to adjust the time.

3. CALCULATION METHOD

As shown in equations (2), (3), and (4), we use the water depth integrated continuity equation and momentum equation in the general coordinate system for basic equations. The definition of each parameter in equations (2), (3), and (4) is shown in equation (5) and (6).

$$J\frac{\partial h}{\partial t}+\frac{\partial}{\partial \xi}\left(\tilde{J}d\eta\cdot U_\xi h\right)+\frac{\partial}{\partial \eta}\left(\tilde{J}d\xi\cdot V_\eta h\right)=0 \tag{2}$$

$$\frac{\partial JhU_\xi}{\partial t}+\frac{\partial JU_\xi U_\xi h}{\partial \tilde{\xi}}+\frac{\partial JV_\eta U_\xi h}{\partial \tilde{\eta}}-J\tilde{J}(V_\eta-U_\xi\cos\theta^{\eta\xi})(U_\xi h\frac{\partial \theta^\xi}{\partial \tilde{\xi}}+V_\eta h\frac{\partial \theta^\xi}{\partial \tilde{\eta}})=J\frac{F_\xi}{\rho}-Jgh\left(\frac{\partial \zeta}{\partial \tilde{\xi}}+\cos\theta^{\eta\xi}\frac{\partial \zeta}{\partial \tilde{\eta}}\right)-J\tau_{o\xi} \tag{3}$$

$$\frac{\partial JhV_\eta}{\partial t}+\frac{\partial JU_\xi hV_\eta}{\partial \tilde{\xi}}+\frac{\partial JV_\eta hV_\eta}{\partial \tilde{\eta}}-J\tilde{J}(U_\xi-V_\eta\cos\theta^{\eta\xi})(U_\xi h\frac{\partial \theta^\eta}{\partial \tilde{\xi}}+V_\eta h\frac{\partial \theta^\eta}{\partial \tilde{\eta}})=J\frac{F_\eta}{\rho}-Jgh\left(\cos\theta^{\eta\xi}\frac{\partial \zeta}{\partial \tilde{\xi}}+\frac{\partial \zeta}{\partial \tilde{\eta}}\right)-J\tau_{o\eta} \tag{4}$$

$$\left(\tilde{J}d\xi,\tilde{J}d\eta\right)=(\Delta\xi,\Delta\eta) \tag{5}$$

$$\tilde{J}=\frac{J}{d\xi\cdot d\eta},\quad \frac{\partial}{\partial \tilde{\xi}}=\frac{\partial}{d\xi\cdot\partial\xi},\quad \frac{\partial}{\partial \tilde{\eta}}=\frac{\partial}{d\eta\cdot\partial\eta} \tag{6}$$

Here, U_ξ, V_η represent the water depth average velocity in ξ,η direction, h is water depth, ζ represents the water surface coordinate, θ is the angle, F_ξ,F_η are the forces in ξ,η direction, J is the Jacobian value, ρ is density, $\tau_{0\xi},\tau_{0\eta}$ are the bed sheer stress in ξ, η direction and g is gravitational acceleration.
Fig. 2 shows the geometric display in a general coordinate system.

In our calculation, the boundary condition at which the discharge at the upstream end is 0 (m^3/s), the downstream water depths are 0.02(m) for Type 1, and 0.107(m) for Type 2. The step time is 0.0001s.

4. RESULT AND DISCUSSION

4.1 Comparison between experimental results and calculation results of wave height in a straight channel

Figures 3 and 4 show the wave height in a straight channel. We discuss the possibility of calculating the wave height in a straight channel using the shallow water equation.

Type 1
At point 1, the wave height profile of the experiment is partially lower than that in the calculation results. It is considered that wave breaking occurred before the bore reached point 1. The experimental values and calculation results roughly agree with each other between points 2 and 4. However, at points 5 and 6, the wave height at the head does not coincide with the calculation. This is because the wave reflection from the sidewall propagates upstream, making the wave height after the head of the bore larger than that in the calculation results.
Type 2
Unlike Type 1, the calculation results express the experimental values. The reflection from the sidewall propagation is not shown at point 6. Particularly, the wave height variation is slightly wavy. It is considered that the condition generated by the bore for Type 2 is almost similar to that of the undular bore.

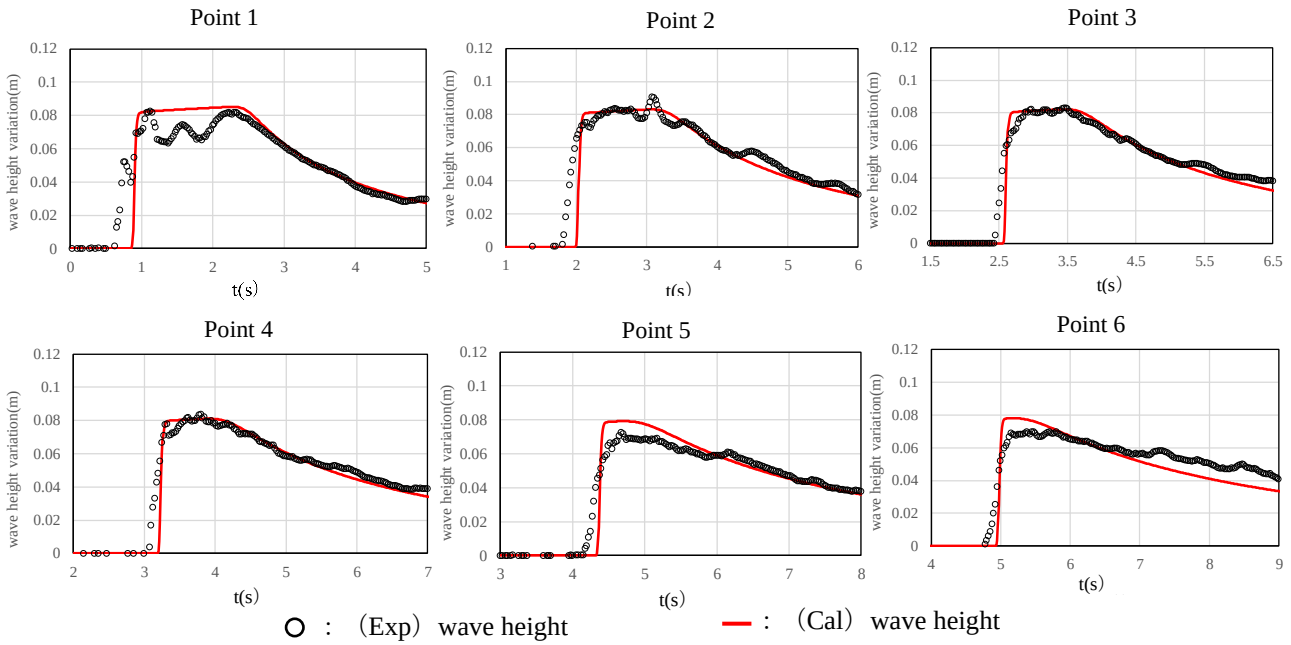

Figure 3. Temporal variation of wave height in a straight channel (*Type 1*)

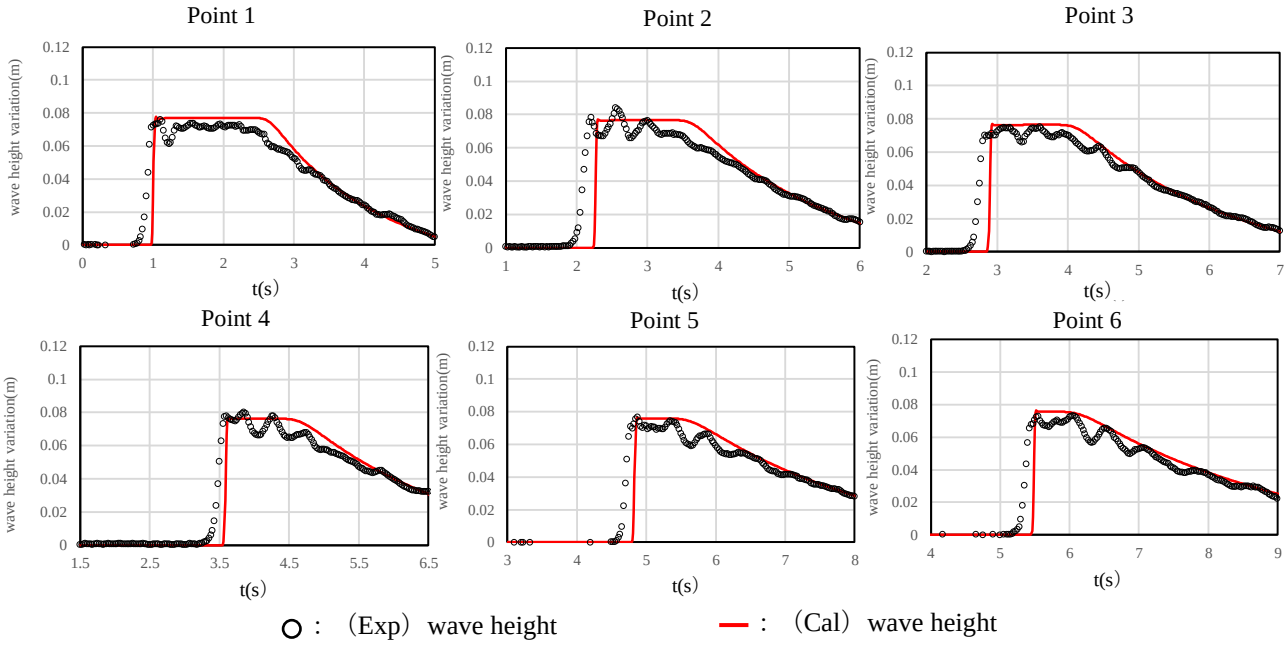

Figure 4. Temporal variation of wave height in a straight channel (*Type 2*)

4.2 Comparison between wave height in a straight channel and meandering channel

Figures 5 and 6 show the experimental results and calculation results of the wave height in a meandering channel. The maximum wave height distribution is shown in Figure 7.

Type 1

The wave height variation at sections 1 and 3 can be reproduced by a two-dimensional calculation. However, for other cross-sections, the calculation and experimental results do not match. In particular, the wave height variation near the outer bank is overestimated, and the difference in water level between the right and left banks cannot be expressed. In the longitudinal distribution of the maximum wave height, the calculation results exceed the experimental values for all cross-sections. Therefore, the breaking bore of Type 1 in the meandering channel cannot be expressed by the two-dimensional shallow water equation.
We use the depth-averaged velocity in our calculation. Therefore, we do not consider the secondary flow caused by the deformation of the vertical velocity distribution. It is considered that the momentum transport caused by the secondary flow leads to the difference in water levels between both banks and the

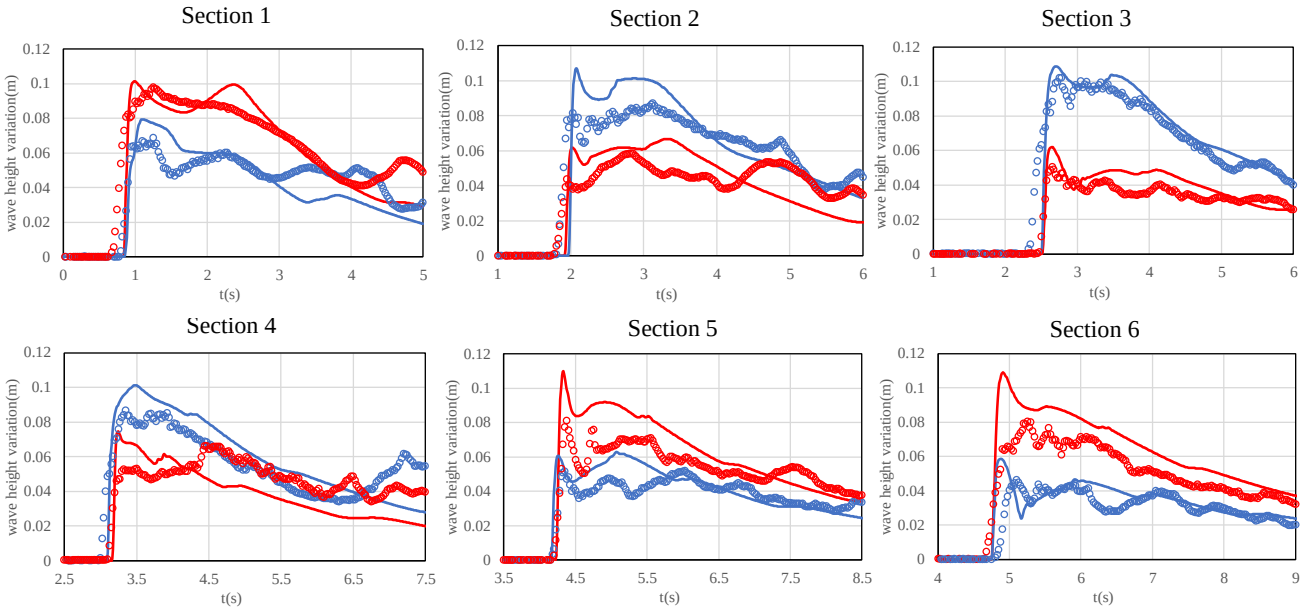

Figure 5. Temporal variation of wave height near both bank (*Type 1*)

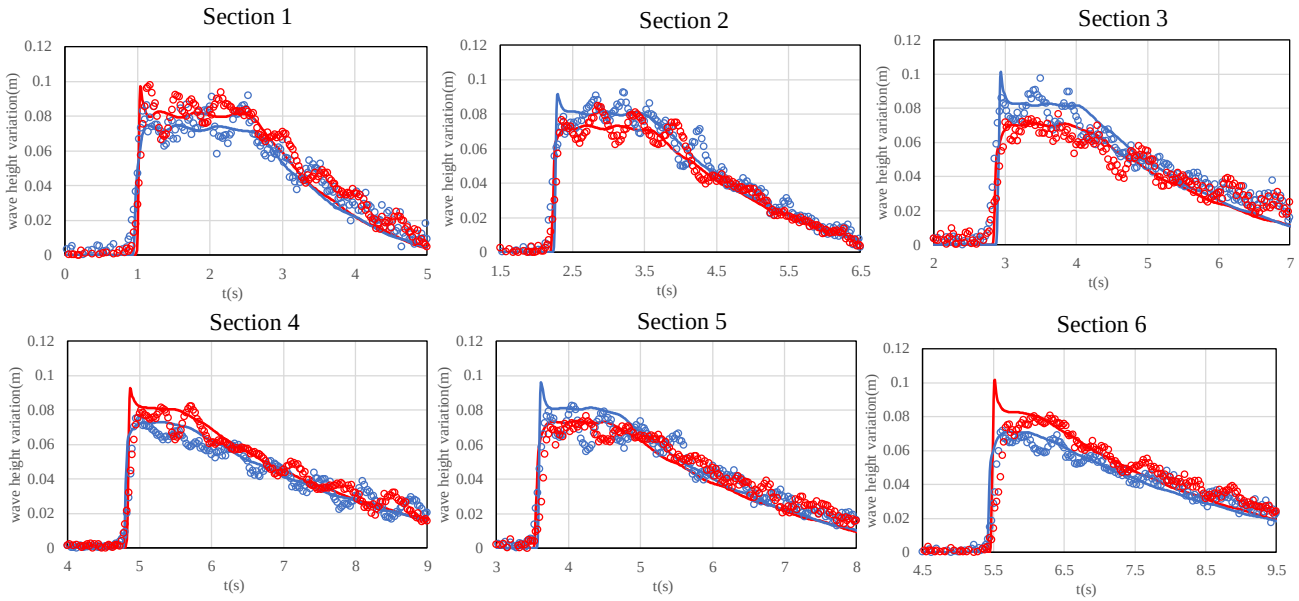

○ : (EXP) the temporal variation of wave height near the right bank from upstream in meandering channel

○ : (EXP) the temporal variation of wave height near the left bank from upstream in meandering channel

— : (CAL) the temporal variation of wave height near the right bank from upstream in meandering channel

— : (CAL) the temporal variation of wave height near the left bank from upstream in meandering channel

Figure 6. Temporal variation of wave height near both banks (*Type 2*)

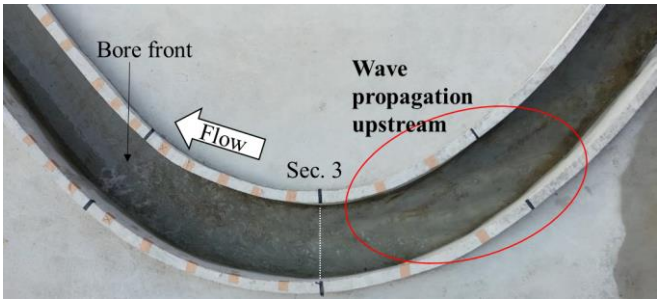

Photo 1. Wave propagation upstream at second curved part (*Type 1*)

overestimation of the outer bank. Therefore, it can be inferred that the type 1 bore in a meandering channel has a strong three-dimensionality of flow. Photo 1 shows the wave propagation upstream – 6-7 s after the gate opening. However, the Fr value is larger than 1 in the calculation at the same time as the experiment. Therefore, from our calculation, the wave cannot propagate upstream. Therefore, it is considered that the reflection from the side wall causes the difference in volume between the experimental and calculated results.

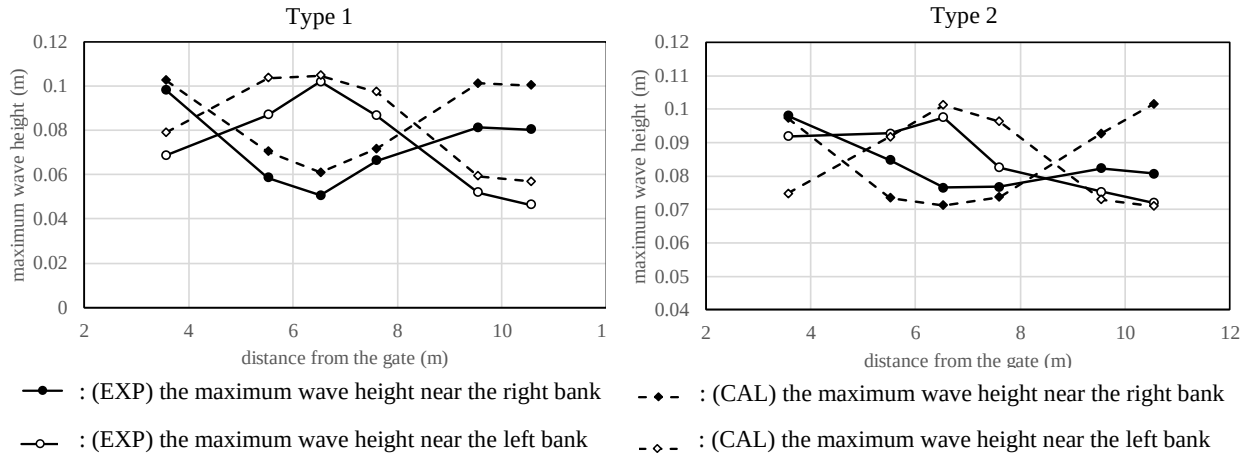

Figure 7. The maximum wave height distribution in a meandering channel

If a huge tsunami strikes when the water level in a river is low, a strong three- dimensional flow may occur. This must be considered to express the effects more accurately.

Type 2

The wave variation near the outer bank at all sections roughly corresponded with the calculation results. It can be inferred that the effect of the deformation of the vertical distribution of the flow velocity on the water level is smaller than that of Type 1. Additionally, soliton fissions, which are seen in the undular bore, are generated. The longitudinal distribution of the maximum wave height indicates that the experimental values are larger than the calculation results on the inner bank, which is probably because of the soliton fission developed on the inner bank and increase in wave height. Therefore, it is found that it can be reproduced more accurately by considering the wave dispersion.

5. CONCLUSIONS

the breaking bore in shallow water depth (Type 1) in a meandering channel, it was investigated that the wave propagation to upstream direction under the supercritical flow condition was induced by the reflection from the side wall, which cannot be expressed in the shallow water equations. As the result, the characteristic of the wave height variation of the Type 1 could not be explained well by the numerical simulation.

The wave height variation of Type 2 (breaking bore in relatively deep-water depth) can be approximately represented by the numerical model. However, unlike Type 1, the maximum wave height increases on the inner bank owing to the development of soliton fission. In addition, the calculation overestimates the maximum wave height on the outer bank.

REFERENCES

Cagatay, H. and Kocaman, S. (2008). Experimental study of tailwater level effects on dam break flood wave propagation, River Flow 2008, *International Conference On Fluvial Hydraulics*, At Izmir, Turkey.

Goto, T. and Syuto, N. (1981). Calculation of tsunami run-up on rivers. *Coastal Engineering Journal*, Vol.28, I_64-I_68.

Guid, L. and Willi, H. H. (1998). Experiments to dambreak wave: Horizontal channel. *Journal of Hydraulic Research*, Vol. 36, 1998 - Issue 3.

Ito, H., Takebayashi, H., Kajiwara, T., Fujita, M. and Tomita, K. (2014). Propagation Characteristics of surges due to landslides in mountainous meandering channel. *Journal of JSCE*, Vol.70, No.4, I_1033-I_1038.

Liu, H. (2017). Experimental Study on Dam-Break Hydrodynamic Characteristics Under Different Conditions, *Journal of Disaster Research*, Vol. 12, Issue 1.

Nakagawa, H., Nakamura, S., Ichihashi, Y. (1969). A study on generation and development of hydraulic bore, Disaster Prevention Research Institute Annuals. B, vol. 12, p543-553.

Sky, M. and Chaudhry, M. H. (1989) Dam-break Flows in Curved Channel. *Journal of Hydraulic Engineering*, Vol. 115, Issue 11.

Soares, S.F and Zech, Y. (2002). Dam break in channels with 90° bend. *Journal of Hydraulic Engineering*, Vol. 128, Issue 11.

Tanaka, N., Yagisawa, J. and Yasuda, S. (2013). Report on Damage Situations by Tsunami Propagation in River Channels and its Overtopping from Embankment in Great East Japan Earthquake. Bulletin of the Faculty of Engineering, Saitama University, Vol.44, I_21-I_24.

Watanabe. A., Fukuoka. S., Mutasingwa. A. G., Ota. M. (2002). The unsteady 2D flow analysis on the deformation of hydro-graph and the flood flow storage in compound meandering channels. *Proceeding of hydraulic engineering*, Vol. 46, pp427-432.

Yung. H. C, Daryl. B. S.(1979). An experimental study of hydraulic and geomorphic changes in an alluvial channel induced by failure of a dam. Water Resources Research, Vol.15, Issue5.